ANNALS OF GEOPHYSICS, 68, 5, DM577, 2025; doi:10.4401/ag-9331
OPEN ACCESS

Impact of the Crustal Velocity Model on Earthquake Location and Moment Tensor Solution: Case Study on the 2025 Aegean Sea Earthquakes

Musavver Didem Cambaz[1]

(1) Boğaziçi University, Kandilli Observatory and Earthquake Research Institute, 34684, Çengelköy, Üsküdar, İstanbul, Türkiye

Article history: received March7, 2025; accepted October 30, 2025

Abstract

The densely populated areas in the Eastern Mediterranean are highly vulnerable to a variety of geohazards, including earthquakes, tsunamis, volcanoes and landslides. The Cyclades archipelago region near Santorini in the Aegean Sea lies within a tectonically active belt capable of generating volcanic activity, major destructive earthquakes and subsequent landslides and/or tsunamis. Understanding the properties of plate boundaries, slabs, active faults and the stress field is crucial for identifying the geodynamic factors driving plate deformation and associated geohazards. A dense seismic network is crucial for precisely locating earthquakes and understanding the active tectonics of the area. In recent years, dense seismic networks such as AdriaArray, have been conducted to provide high quality data for imaging crustal and upper mantle structure, as well as analysing seismic activity in the Mediterranean region. This study focuses on the computation of a 1D velocity model in order to improve the earthquake parameters in the region. Taking advantage of recent deployments, dense station coverage, and a comprehensive earthquake catalogue from recent seismic activity in the Cyclades archipelago, Aegean Sea, a new 1D crustal velocity model was developed and compared with existing models in the region. The presented results emphasize the influence of the crustal velocity model on earthquake parameters and moment tensor solutions, with strong potential to enhance forthcoming investigations into source mechanisms, fault kinematics, and seismic velocity structures in the Aegean Sea.

Keywords: Aegean Sea, Seismicity, Earthquake Catalog; Moment Tensor Solution; Crustal structure; 1D Velocity Model, AdriaArray

1. Introduction

Seismic networks form the backbone of earthquake detection systems, providing invaluable data for studying the Earth's structure, the behaviour of tectonic plates, hazard and risk assessment, real-time monitoring and response, tsunami warning systems, scientific research, and public awareness. These are essential for detecting and monitoring earthquakes, particularly along tectonic plate boundaries where seismic activity is most intense.

In regions where national borders limit a single country's ability to achieve sufficient azimuthal coverage – the directional distribution of seismic stations around an earthquake's epicenter – international cooperation and data-sharing protocols become critical. The significance of large seismic deployments in these regions cannot be overstated, as they provide essential data for understanding Earth's dynamics, mitigating disaster risks, and safeguarding human lives and infrastructure. Dense regional passive broadband seismic experiments, such as AdriaArray (Kolinsky et al., 2025), AlpArray (Hetényi et al., 2018), EGELADOS (Brüstle, 2012), and SIMBAAD (Salaün et al., 2012) have been conducted across the greater Alpine and Mediterranean regions. These projects play a crucial role in providing high-quality data for imaging the crustal and upper mantle structure, as well as analysing seismic activity through advanced analysis tools. These large seismic networks and well distributed seismic stations also provide very well constrained earthquake location parameters which is essential for most of the seismological, earthquake hazard and risk mitigation studies. Beside the seismic network properties (such as network density, station distribution, closest station-distance, azimuthal coverage etc.), initial velocity models are one of the other factors affecting the resultant earthquake parameters. An inaccurate velocity model can introduce significant errors, such as mislocating the epicenter, biasing depth estimates or distorting the focal mechanism obtained from moment tensor solutions. 1-D velocity models are essential for many studies especially in precisely modelling earthquake mechanisms, fault plane solutions (Carvalho et al., 2018; Turhan et al., 2018; Antunes et al., 2020) and hence earthquake and tsunami hazard and risk mitigation studies etc.

At the end of January 2025, a seismic activity started near Santorini in the Cyclades island complex (South Aegean Sea) and was followed by a high social impact not only in Greece but also in Türkiye. The activity was clustered within a narrow area in the SW-NE trending zone, approximately 30 km in length and ~18 km in width (Triantafyllou and Papadopoulos, 2025) corresponding to the southern side of the rupture zone of the very large tsunamigenic Amorgos earthquake (Mw7.7) (Papadopoulos and Pavlides, 1992; Okal et al., 2009). The maximum magnitude was M5.3, (up to the date 2025-02-10 20:16:28 UTC) according to the NOA catalog (https://bbnet.gein.noa.gr/HL/databases/database). The focal depths of the earthquakes varied, though they remained within a shallow range (up to 20 km). Thanks to the urgent protective countermeasures of the civil protection authorities of the country, thousands of people were evacuated from the nearby islands in Greece. The Disaster and Emergency Management Authority (AFAD) of Türkiye convened a high-level meeting and boosted precautions amid Aegean Sea Seismic Activity (https://www.turkiyetoday.com/turkiye/turkiye-holds-emergency-meeting-on-santorini-seismic-activity-potential-risks-116926/).

Precisely determined earthquake parameters are important not only for understanding the seismicity and seismotectonics of a region, but also for providing an accurate estimation of the seismic hazard and risk parameters, trustful focal mechanism solutions (Cambaz and Mutlu, 2016; Turhan et al., 2018, Acarel et al., 2019; Antunes et al., 2020). For faster and more robust ray tracing in 1D velocity models and also due to the lack of reliable 3D models most seismological centers use 1D velocity models for the routine earthquake locations (Husen et al., 2011; Kianimehr et al., 2018; Cambaz et al., 2019). This study aims to develop a new 1D crustal velocity model for the Cyclades region in the Aegean Sea. Utilizing recent station deployments, dense network coverage, and a high-quality earthquake catalog from the National Observatory of Athens (NOA), a region-specific velocity model was computed using the VELEST algorithm. The resulting model was compared with existing models derived from previous seismic experiments. The findings demonstrate the influence of the velocity model on earthquake parameters and moment tensor solutions, offering valuable insights for future studies on source mechanisms, fault kinematics, and seismic velocities in the Aegean Sea.

2. Tectonic Overview

The Eastern Mediterranean is one of the most seismically active and rapidly deforming region in Europe (McKenzie, 1972, 1978; Le Pichon and Angelier, 1979; Dewey et al., 1986; Jackson and McKenzie 1988; Taymaz et al., 1990, 1991; Ambraseys and Jackson 1990; Reilinger et al., 2006). As a result, it has been the target of many geophysical studies due to its active tectonics and very high rate of seismicity. Continuous regional deformation along the seismically active boundaries gives rise to a variety of geologic structures such as suture zones, metamorphic complexes and young orogens (Stampfli, 2000). Significant variations exist on the tectonic styles and crustal structures. Eastern Anatolia and Western Anatolia can be very roughly represented by two different velocity models: one with a thinner crust for western Türkiye and the other with a relatively thicker crust covering eastern Türkiye

(Saunders et al., 1998; Delph et al., 2015) also in line with the Earth models and seismic velocities at (Cambaz, 2010, Cambaz and Karabulut, 2010).

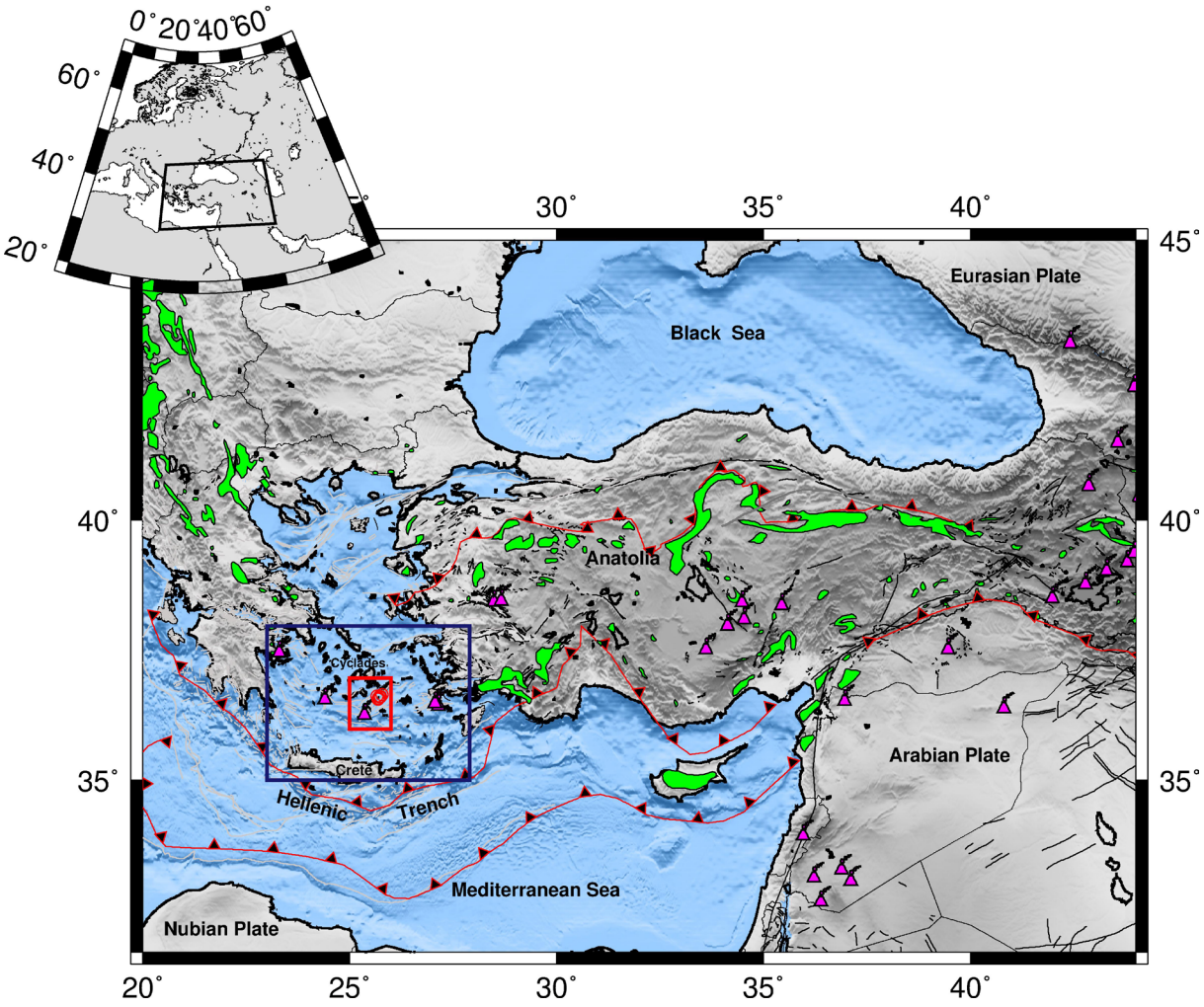

Figure 1. Tectonic setting of the Eastern Mediterranean region modified from Stampfli (2000); Okay and Tuysuz (1999); Robertson (2000); Tatar et al. (2000), Cambaz (2010), Cambaz and Karabulut (2010). Bathymetry and Topography of the region are derived from ETOPO5 and GTOPO30. Black lines represent the active faults in Türkiye (Emre et al., 2013; 2018). Grey lines indicate NOA faults (NOAFAULTS: Ganas et al., 2013; 2018; 2023; https://zenodo.org/records/13168947).

The Hellenic Trench (Fig. 1) in the eastern Mediterranean is the most seismically active region in Europe (McKenzie, 1972; Papazachos, 1977). The broader Aegean Sea area and surroundings are characterized by high seismicity and complex tectonics dominated by the convergence of Nubia with Anatolia and Aegea (Howell et al., 2017). The closure of the Tethys oceanic basins in the region resulted in crustal thickening and consequent post-orogenic extension and magmatism (Pavlides et al., 2024) which is reflected in significant variations of crustal thickness. The tectonic structure is mainly characterized by northward subduction of the African slab beneath the Aegean plate at a rate of 4 cm/yr (McKenzie, 1978; Reilinger et al., 2006), leading to extensional strain and crustal thinning (25-27 km) in the southern Aegean. This process is evidenced by seismic reflection profiles (Makris, 1978; Bohnhoff et al., 2001), receiver function analysis (Sodoudi et al., 2006), gravity analysis (Tirel et al., 2004), and tomographic studies (Drakatos et al., 1997; Papazachos and Nolet, 1997; Karagianni et al., 2002, 2005; Karagianni and Papazachos, 2007; Endrun et al., 2008; Papazachos et al., 2020). Shallow seismicity is concentrated in the upper crust (depths <15-20 km) along the northern Santorini-Amorgos graben (Bohnhoff et al., 2006; Brüstle, 2012).

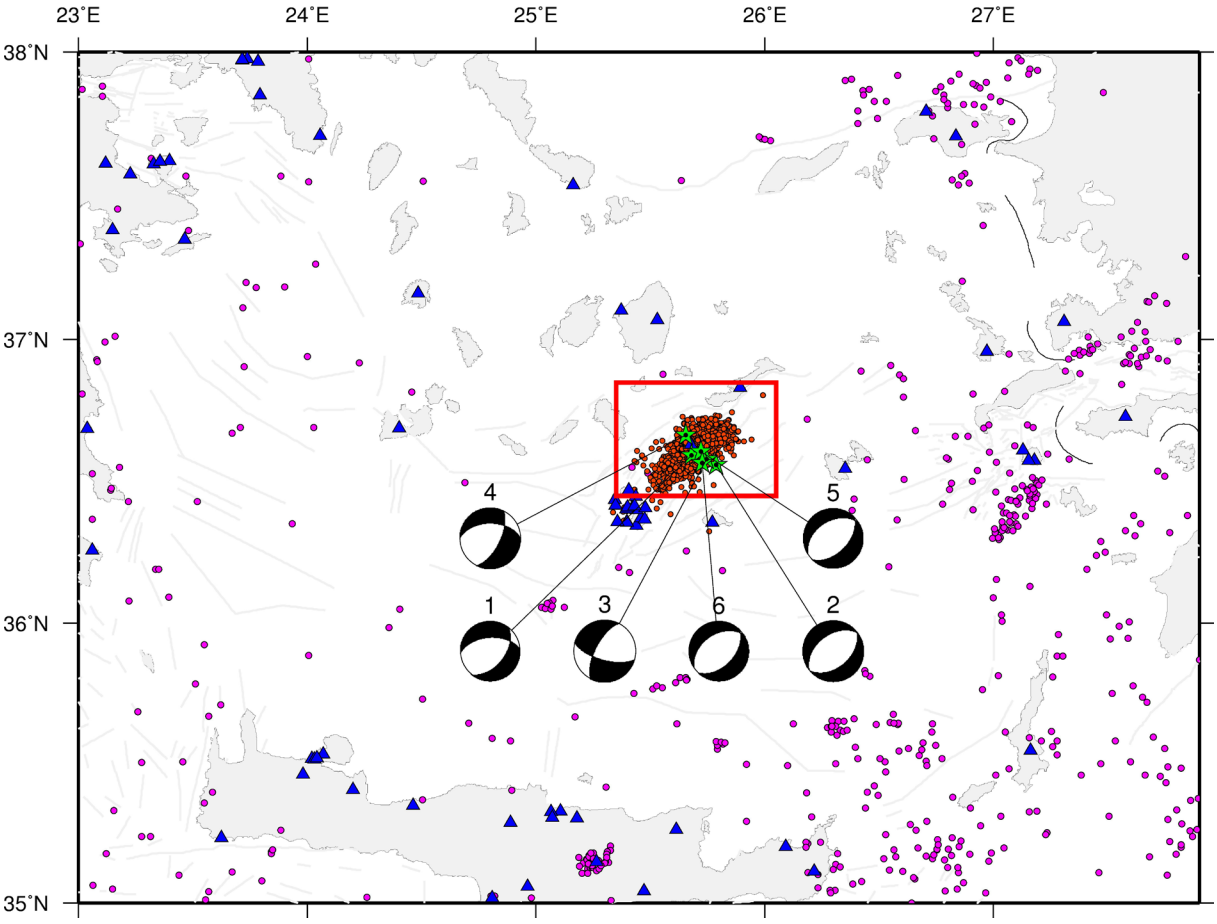

Figure 2. Seismicity map of the region. Purple circles indicate the earthquakes with M ≥ 4.0 reported in the NOA catalog between 2025.01.01-2025.02.15 in the region. Red circles indicate the earthquakes with M ≥ 0.1 and green stars indicate the M ≥ 5.0 earthquakes (R = 100 km, Lat = 36.50N, Lon = 25.50E; red rectangle). Blue triangles are the seismic stations (EIDA NOA; https://eida.gein.noa.gr/). Beachball Moment Tensor Solutions were computed by NOA (https://bbnet.gein.noa.gr/HL/seismicity/mts). Grey lines indicate faults reported in the NOAFAULTS database (Ganas et al., 2013; 2018; 2023; https://zenodo.org/records/13168947).

In many studies, the region is stated as one of the most seismically active regions in Europe. According to the NOA catalog 748 earthquakes (M ≥ 4.0) were recorded in the region between the 01.01.2008-15.02.2025 (Fig. 2). These are mainly recorded in the eastern sector (Lon > 25.00E). Episodic intense earthquake swarms have been observed in the region mainly in the Cyclades island complex (Bohnhoff et al., 2006; Brüstle, 2012). During the recent earthquake activity beginning from January 2025, more than 2500 earthquakes (M ≥ 0.1) occurred in the region (R = 100 km, Lat = 36.50N, Lon = 25.50E) (Fig. 2). Until the 15.02 2025, six of these earthquakes were bigger than 5, the strongest of which reached a magnitude of M5.3 on 10.02.2025 (Table 1). This earthquake activity near Santorini continued to perplex scientists, keeping disaster risk management teams, civil protection authorities and the general public on high alert and in a state of suspense. Reports of the seismic activity had garnered global attention. Santorini activity was reported by many institutes and agencies (AFAD: https://deprem.afad.gov.tr/assets/pdf/ege_denizi.pdf; EMSC: https://emsc-csem.org/Special_reports/?id=351; UNESCO-IOC: https://www.unesco.org/en/articles/santorini-ongoing-earthquake-swarm; https://emsc-csem.org/Special_reports/?id=351; KOERI: http://www.koeri.boun.edu.tr/sismo/2/santorini-adasi-ege-denizi-deprem-etkinligi-10-2/; METU: https://tinyurl.com/3hrcnh6z).

Table 1. Earthquakes M > 5.0 in NOA catalog between the dates at 2025.01.01-2025.02.15 in the region (R = 100 km, Lat = 36.50N, Lon = 25.50E) (Lat, Lon, D, M refers to Latitude, Longitude, Depth and Magnitude, respectively).

Date/Time* (UTC)	NOA (Lat, Lon, D, M)	EMSC (Lat, Lon, D, M)	GFZ (Lat, Lon, D, M)	KOERI (Lat, Lon, D, M)	USGS (Lat, Lon, D, M)
20250204 13:04:14	36.61, 25.70, 12.8, 5.0	36.56, 25.61, 8.0, 5.2	36.61, 25.62, 7.0, 4.9	36.59, 25.53, 5.3, 4.9	36.52, 25.57, 16.2, 5.3
20250205 19:09:38	36.64, 25.74, 12.0, 5.2	36.65, 25.64, 10.0, 5.1	36.63, 25.70, 5.0, 5.2	36.56, 25.56, 8.0, 5.2	36.61, 25.64, 10.0, 5.1
20250209 19:05:39	36.64, 25.65, 12.1, 5.0	36.66, 25.60, 15.0, 5.2	36.64, 25.64, 7.0, 5.1	36.56, 25.56, 5.0, 5.2	36.69, 25.62, 10.0, 5.2
20250210 20:16:28	36.68, 25.78, 11.8, 5.3	36.69, 25.71, 8.0, 5.2	36.67, 25.70, 8.1, 5.2	36.56, 25.56, 8.1, 5.2	36.69, 25.67, 10.0, 5.2
20250210 22:37:26	36.64, 25.72, 13.3, 5.0	36.64, 25.65, 8.0, 5.1	36.56, 25.56, 10.1, 5.1	36.56, 25.56, 10.1, 5.1	36.63, 25.62, 10.0, 5.1
20250212 01:14:54	36.59, 25.68, 11.8, 5.0	36.56, 25.62, 10.0, 5.1	36.60, 25.63, 6.0, 5.1	36.56, 25.56, 10.1, 5.1	36.56, 25.55, 10.0, 5.1

*Date/Time (UTC) of the earthquakes listed according to the NOA catalog and location parameters of these events from the KOERI, EMSC, GFZ, KOERI, USGS.

3. Data

This study benefits from two data strengths: the high quality and dense station coverage and second, the amount of recorded earthquakes due to the recent seismic activity in the study region. The Hellenic Unified Seismic Network (HUSN) represents the seismic networks that monitor earthquake activity in the Aegean Sea and mainland Greece as a result of the merging of three networks operated by Greek universities (Athens, Thessaloniki and Patras) with the nationwide network operated by the National Observatory of Athens (NOA) (Konstantinou, 2018). During the AdriaArray Seismic experiment the station density was strengthened with the installation of 31 new portable stations where the station density of the Hellenic Unified Seismic Network (HUSN) was low (Sokos et al., 2023). Comprehensive information on the seismic data from Greece is available in Evangelidis et al. (2021), and details on the AdriaArray station installations, including availability plots and noise analyses, are presented in Sokos et al. (2023) (Fig. 2).

A significant seismic crisis has been affecting the Santorini-Amorgos region since January 2025. By 15 February, approximately 2500 earthquakes with magnitudes up to 5.3 had been recorded, including six earthquakes with Mw ≥ 5.0. The seismicity was primarily concentrated about 25 kilometers northeast of Santorini and 25 kilometers southwest of Amorgos islands. For this study, a database was compiled using the earthquake catalog of the National Observatory of Athens (NOA) (https://bbnet.gein.noa.gr/HL/databases/database). Phase readings of earthquakes with M ≥ 3.5 were collected for the time interval between 01.01.2025 and 15.02.2025 for the region within a 100 km radius centered in 36.50N, 25.50E. IMF formatted data were converted to SEISAN (Ottemöller and Havskov, 2013) format for this study.

As one of the fundamental principles of seismology, James et al. (1969) emphasized that station spacing plays a crucial role in accurately determining earthquake locations. Although the distribution of stations is often constrained by geographical conditions, the ANYD station – situated near the center of the earthquake sequence - was the closest to the event origins, with some earthquakes occurring less than one kilometre away (Fig. 3). On average, the distance between the ANYD station and the events was approximately 4.5 km. According to James et al. (1969), accurately determining the depth of shallow earthquakes becomes difficult when their depth is less than about half of the mean station spacing, even if they occur within the network, unless they are located very close to a station. The presence of the ANYD station, owing to its strategically significant location, greatly enhances the accuracy of earthquake location estimates in the region.

Gomberg et al. (1990) examined the key factors influencing accurate hypocentre determination and pointed out the critical role of recording S phases at seismic stations located within approximately 1.4 times the focal

depth from the earthquake source. The constraints proposed by Gomberg et al. (1990), was considered as one of the most important criteria in data selection. The quality of the velocity model derived using VELEST largely depends on the accuracy of earthquake locations in the selected catalog which in turn is strongly influenced by the number of observations, as well as the distance and distribution of stations. Accordingly, the earthquakes included in the inversion were selected based on the following criteria;

- The number used stations should be more than 8 with at least two S phases,
- The azimuthal gap should be less than 160°,
- The RMS residual should be less than 0.5,
- The distance to the nearest station does not exceed one focal depth.

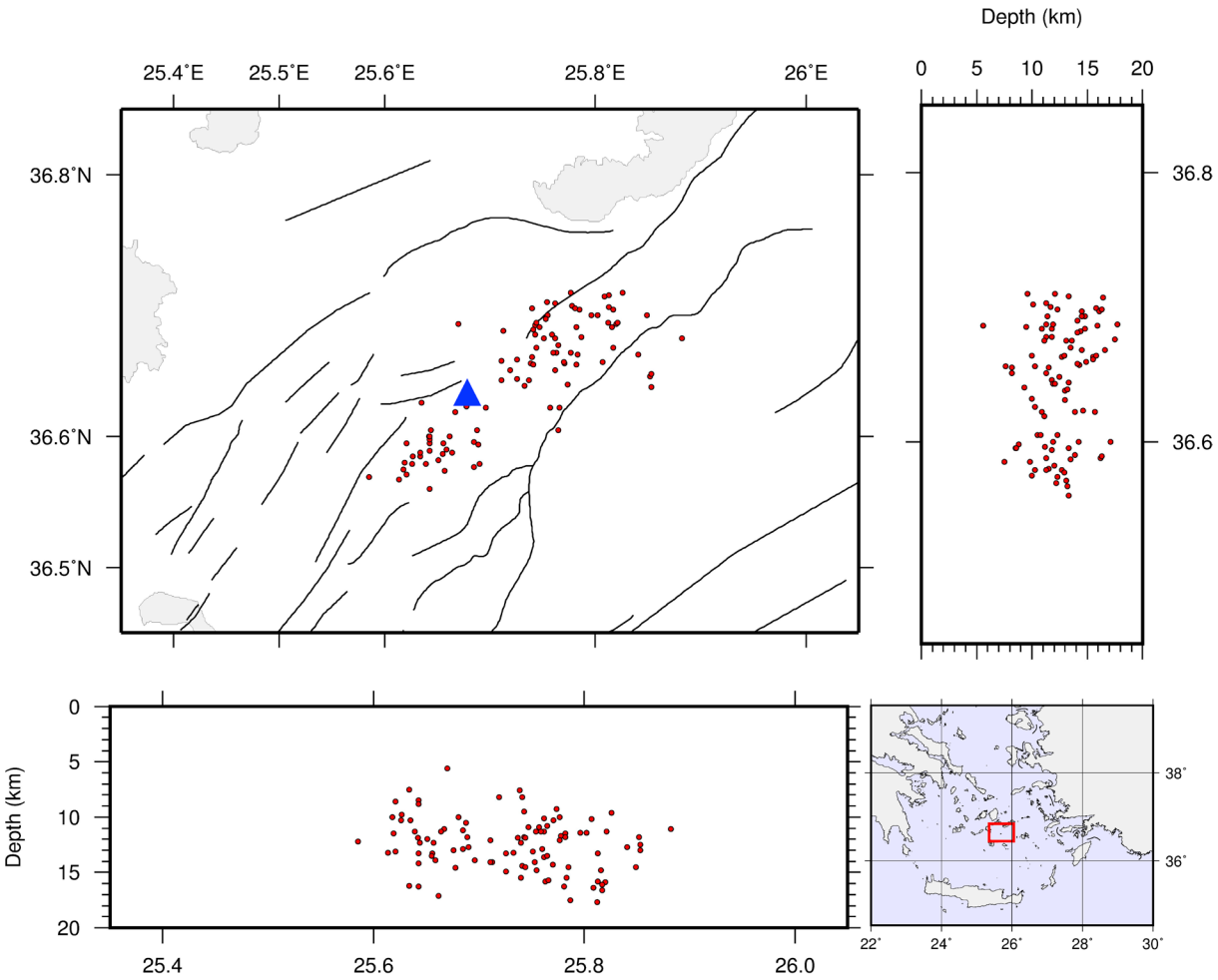

Figure 3. Seismicity map for the region from NOA catalogue recorded in between 3 February 2025-15 February 2025, including the earthquakes (red) selected for this study according to the criteria summarized in section 3. Blue triangle shows the closest station ANYD, located on the Anydros island. Black lines indicate NOA faults (NOAFAULTS: Ganas et al., 2013; 2018; 2023. https://zenodo.org/records/13168947

Overall, the NOA catalog was highly accurate and well-located, with RMS values consistently below 0.5. More than 600 earthquakes were evaluated in terms of their residuals, first station distances, number of P and S phases readings by using HYPOCENTER earthquake location code of SEISAN (Lienert et al., 1986; Lienert and Havskov, 1995, Havskov and Ottemöller, 1999). According to the results of these test models, minimum rms values were selected for a further detailed investigation. To build the database, key parameters such as the source distance to the closest station, azimuthal gap, and the number of phase readings were taken into account. Prior to February 3rd, the source distance to the first station typically exceeded 20-25 km. However, with the addition of the ANYD station

(http://www.geophysics.geol.uoa.gr/stations/archive/qplotstation.php?station=ANYD&net=HT&lng=en), the closest station distance decreased significantly. As a result, earlier earthquake readings were excluded from the analysis for estimating the 1D velocity model. A total of 409 earthquakes were utilized for the computation of the minimum 1D velocity model.

4. Method

The software package VELEST (Kissling et al., 1994, Kissling, et al., 1995) was used in this study to obtain a minimum 1D velocity model defined as the velocity model that produces the smallest uniform error for the set of events with well constrained locations (Kissling, 1988; Kissling et al., 1994). VELEST simultaneously inverts P and S wave travel time readings for a 1D velocity model, station delays and hypocentral locations of earthquakes. First solves the forward problem by tracing direct reflected and refracted rays from source to receiver and then uses the standard damped least square solutions for the inverse problem. It is important to have a well-determined specific velocity model for the enhanced seismic studies in a region. An accurate velocity structure information will result in precise epicenter and depth determination and thus presents a focused picture of seismotectonic structures. The most critical factor for the linearized inverse problem, already stated by several authors (Kissling, 1988; Thurber, 1992; Kissling et al., 1995), is the dependence on the initial velocity model that affects the final solution. Here, we address this problem by exploring different 1D initial velocity models, from previous studies (Novotny et al., 2001, Drakatos et al., 2002; Bahnhoff et al., 2006; Brüstle et al., 2012) in the proximity of the study area.

Before reaching the optimum solution for the velocity model, one hundred velocity models were calculated (Fig. 4). These models were computed by random positive and negative velocity perturbations to each layer of the initial velocity model, allowing exploration of a broad range of possible velocity structures. Repeating this procedure five times, 500 models were computed and tested simultaneously inverting P and S wave travel times for a 1D velocity model, station delays and hypocenters of earthquakes. The earthquakes are relocated by using the best velocity model and station corrections. Out of five hundred runs used for each initial velocity models, we choose a final velocity model that represents the best trade-off between station delays and root mean square (rms) residual error. The 1-D output models computed for each data set show the resultant minimum RMS values: 0,351. One dimensional P and S wave velocity models are developed using the selected data-set and the earthquakes are relocated by using the obtained local velocity model. Figures 5 and 6 present the relocated earthquakes obtained using the computed 1D velocity model, with Fig. 5 showing the selected events and Fig. 6 displaying the full initial catalog without elimination. Results indicate that the hypocentral depths of the re-located earthquakes are shallower (green circles).

Intense earthquake activity in the Aegean Sea and the dense seismic instrumentation in the region provided the opportunity to achieve a well located earthquake catalog for this study. 409 well-located earthquakes were selected for the database in order to compute a minimum 1D velocity model for the region. Approximately, 22 000 phase readings (including 16078 P phase readings at almost 200 seismic stations 5924 S phase readings) were used for the calculation of the velocity model. Station corrections are an essential component in the computation of a 1D velocity model, as they account for the influence of local geological effect. Negative station corrections indicate higher seismic velocities, whereas positive corrections suggest lower velocities relative to the crust beneath the reference station. In order to calculate station corrections, we used station ANYD as the reference station due to its abundance of phase readings; (802 with 408 P phases and 394 S phases) and its favourable location at the center of the network (Fig. 7).

The earthquakes were relocated using the optimal velocity model together with station corrections derived from the observed travel-time delays. Station corrections constitute an essential component of the 1D velocity model, as they account for the geological effects. Negative station corrections indicate higher local velocities, whereas positive corrections reflect lower velocities relative to the crust beneath the reference station. A negative correction implies that the observed travel times are shorter than those predicted by the model, meaning the actual seismic velocities are higher than those represented in the reference model. Additionally, the network's margin causes larger time corrections (Brüstle, 2012). Figure 7 represents lower station corrections at the southern part of the reference station, (Anydros) and higher station corrections indicating higher velocities in the northern part of the reference station.

Table 2. The input velocity models adapted from Novotny et al. (2001), Drakatos et al. (2002), Brüstle (2012) which has been tested during this study.

Novotny et al. (2001)		Drakatos et al. (2002)		Brüstle A. (2012)	
Depth (km)	P wave velocity (km/s)	Depth (km)	P wave velocity (km/s)	Depth (km)	P wave velocity (km/s)
0.0	2.31	0.0	4.50	<5	5.74
1.0	4.27	3.0	5.10	5-10	5.89
2.0	5.52	4.0	5.60	10-15	5.89
5.0	6.23	8.5	5.80	15-20	5.91
16.0	6.41	12.0	6.00	20-25	6.23
33.0	8.37	20.0	6.50	25-30	6.26
		30.0	7.00	30-35	7.53
				35-40	7.55

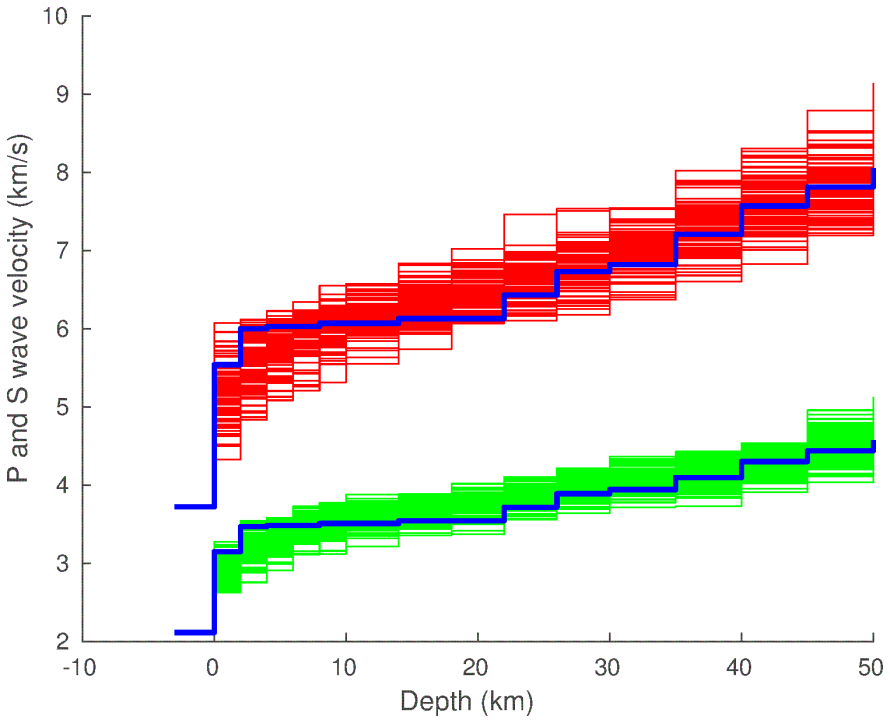

Figure 4. 1-D initial P wave (red) and S wave (green) velocity models were randomly generated from the input velocity model (blue) to compute the optimum velocity model for this study.

Table 3. Final 1D P-Wave velocity model obtained for the study area.

Depth (km)	Vp (km/s)	Vs (km/s)
0.0	4.85	2.79
2.0	5.37	3.15
6.0	6.16	3.63
14.0	6.17	3.63
18.0	6.59	3.83
26.0	6.70	3.91
30.0	7.63	4.26
35.0	7.70	4.27
40.0	7.93	4.31
45.0	7.95	4.36
50.0	8.03	4.62

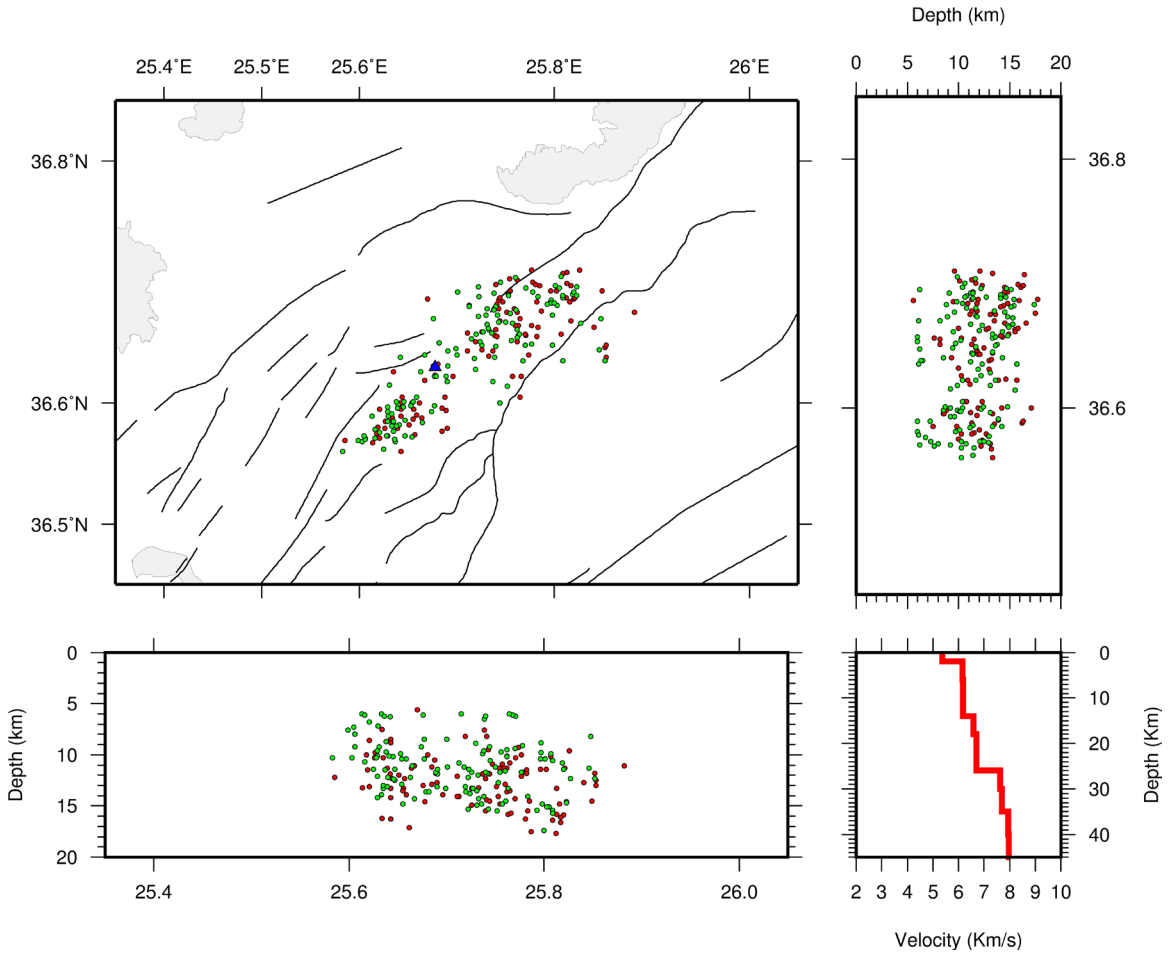

Figure 5. 409 events selected for the P-wave and S-wave inversion. The final hypocentre locations of the earthquakes are presented. Red circles indicate the input and green circles indicate the output hypocenters obtained with the computed velocity model in this study. A latitudinal depth section is shown on the right side, and a longitudinal depth section is plotted along the bottom. The minimum 1-D model used in the computation is presented in the lower right corner (Table 2). The blue triangle represents the closest station ANYD, located on the Anydros island. Black lines indicate NOA faults (NOAFAULTS: Ganas et al., 2013; 2018; 2023, https://zenodo.org/records/13168947).

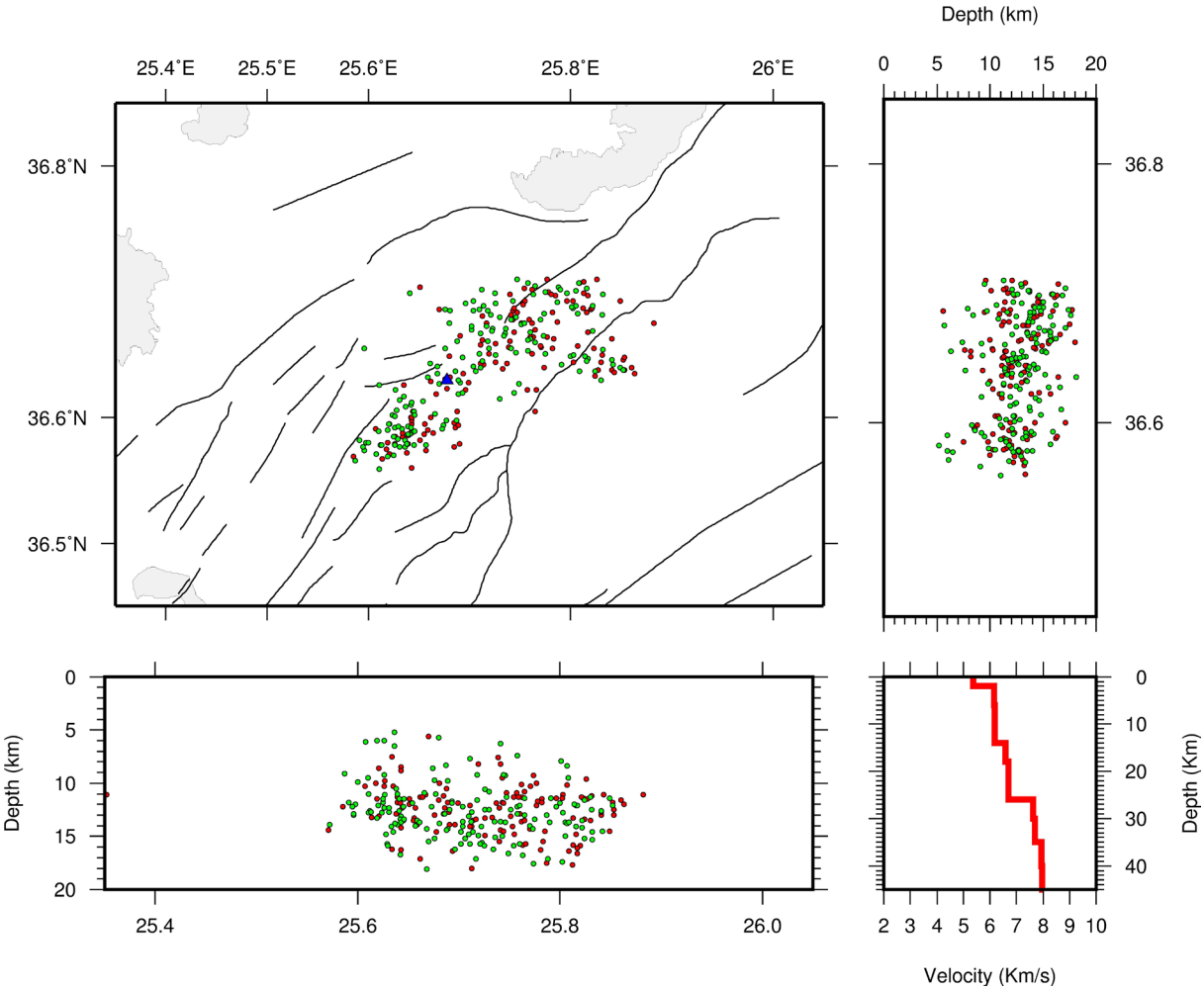

Figure 6. The final hypocentre locations of the events relocated with the computed velocity model for the region. Red circles indicate the input and the green circles indicate the output hypocenters with the computed velocity model in this study. A latitudinal depth section is shown on the right side, and a longitudinal depth section is plotted along the bottom. The minimum 1-D model used in the computation is presented in the lower right corner (Table 2). The blue triangle shows the closest station ANYD, located on the Anydros island. Black lines indicate NOA faults (NOAFAULTS: Ganas et al., 2013; 2018; 2023, https://zenodo.org/records/13168947).

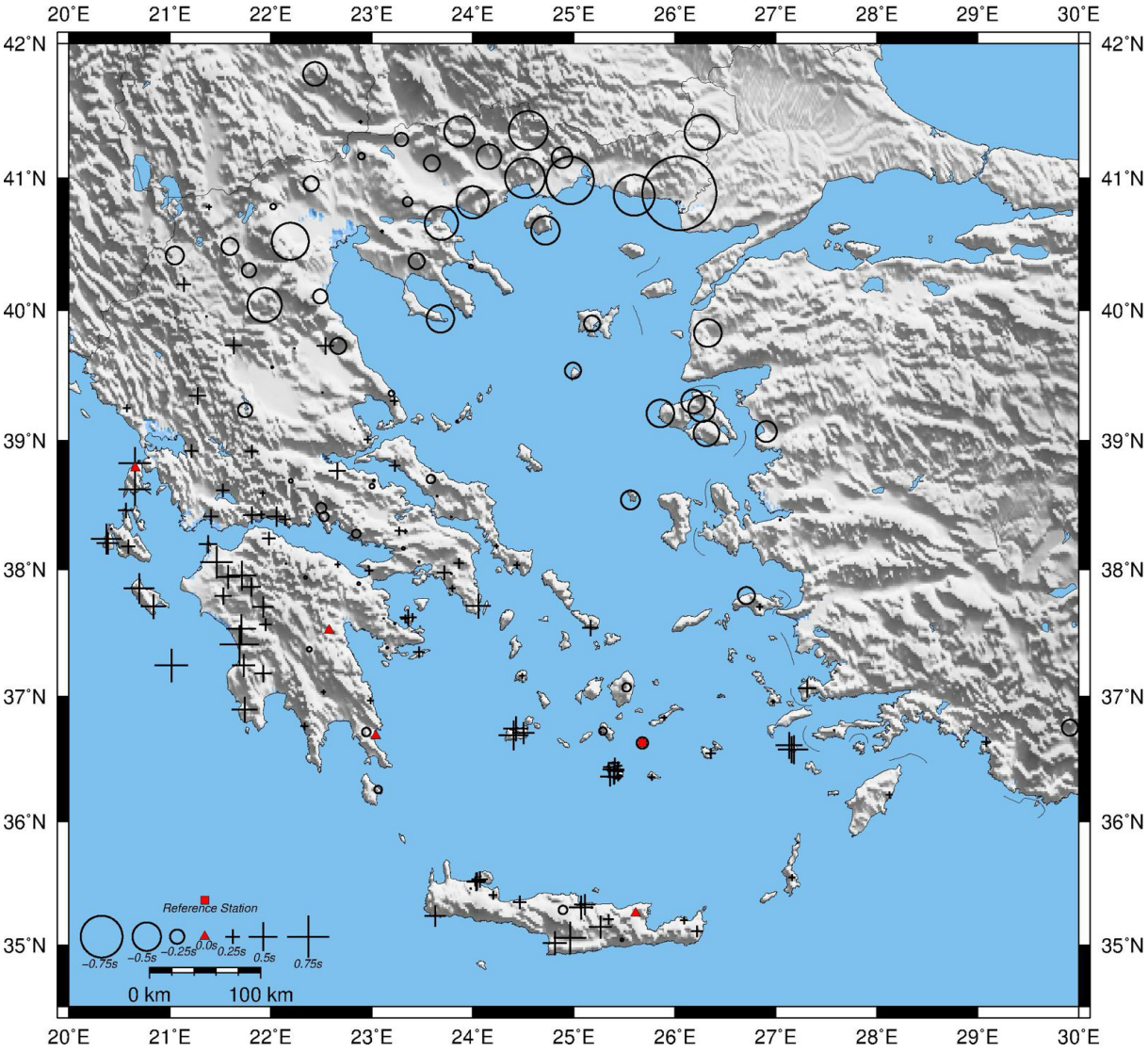

Figure 7. P-wave station corrections for the final 1-D P-wave velocity model. Crosses and circles on the map show the positive and negative station delays relative to the reference station, respectively. The reference station (ANYD) is marked by a red square.

Histogram illustrates the hypocentral depths distribution of the input catalog a) input hypocentral depths (a) and the output hypocentral depths distribution obtained with the velocity model derived in this study (b). The depth distribution in Fig. 8b appears more consistent and less dispersed, indicating improved stability in event localization. This improvement can be attributed to the very close first station distances, the favorable station distribution, and the abundant number of high-quality phase readings, all of which enhance the accuracy of travel-time inversions and lead to a more constrained estimation of focal depths.

Some further investigations were performed to see the differences of results with various velocity models. To compare the differences in the parameters such as depth, rms, erh, erz results of the models compared in Fig. 9. The outputs of the previously mentioned Novotny et al. (2001), Drakatos et al. (2002), Brüstle (2012) velocity model presented together with the model computed in this study. The comparison of results across different velocity models demonstrates clear improvements when using the model developed in this study. In the Novotny et al. (2001) model, earthquake depths mostly cluster between 5-10 km, indicating relatively shallow seismicity. RMS residuals are concentrated around 0.4-0.5 s, while ERH and ERZ values range mainly between 2-3 km, suggesting moderate location uncertainties. The Drakatos et al. (2002) model, in contrast, yields systematically deeper focal depths (15-18 km), implying a velocity model with higher crustal velocities or different layering. The RMS values (0.4-0.6 s) are slightly higher than in Novotny's results, while ERH and ERZ values

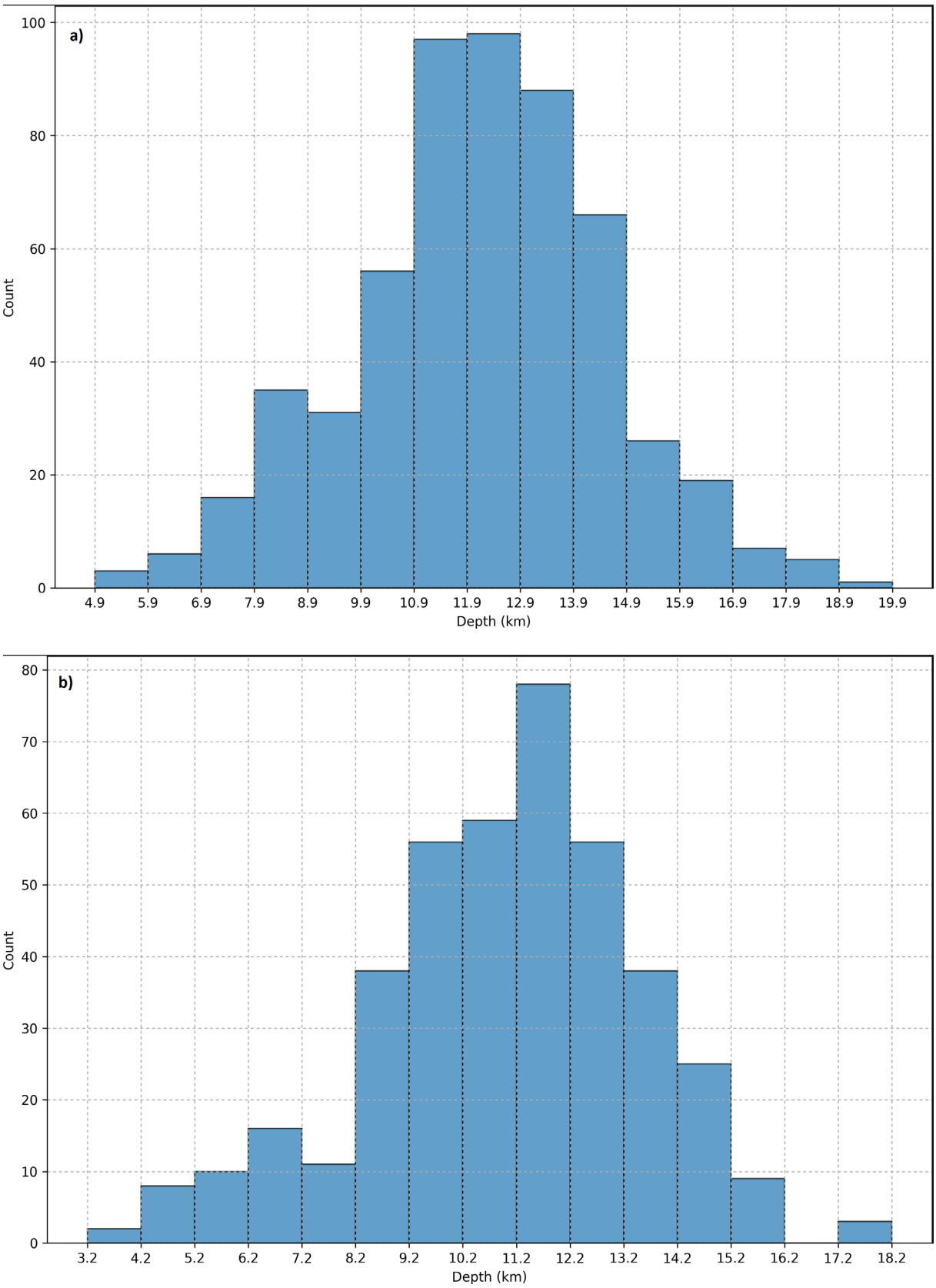

Figure 8. Hypocentral depth histograms. Figure 8a indicates the depth distribution of the input catalog. Figure 8b indicates the depth distribution estimated with the obtained velocity model in this study.

a) Novotny et al. (2001)

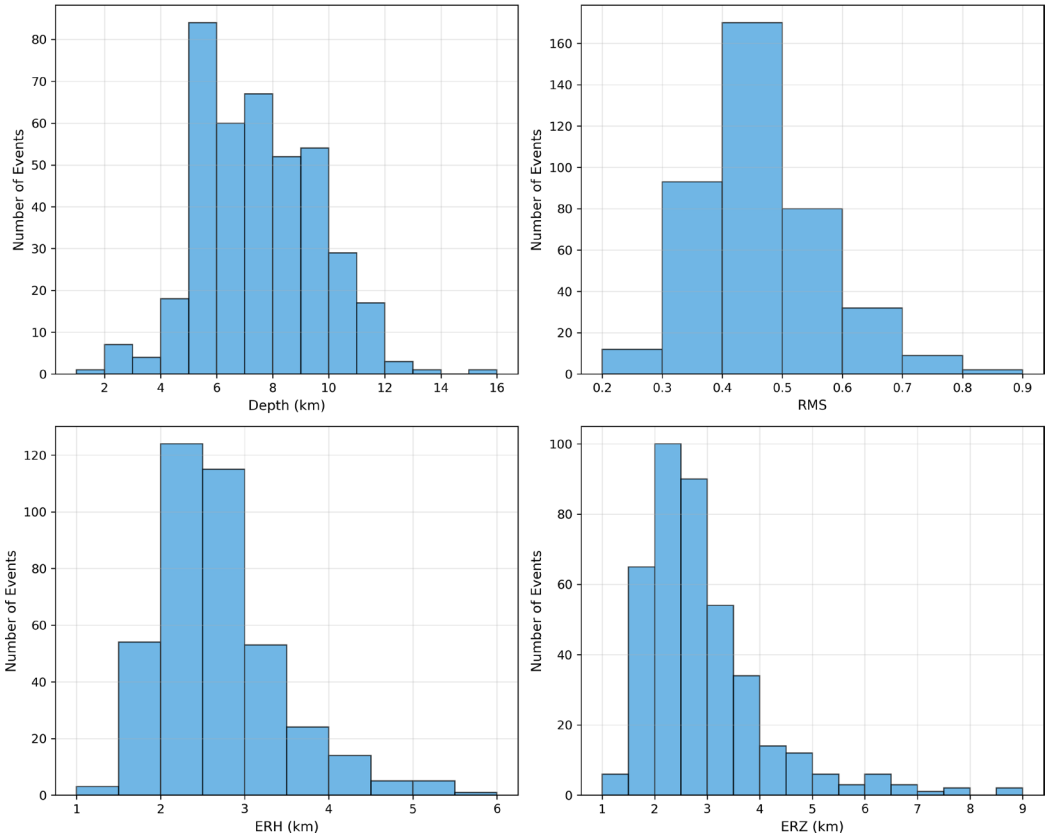

b) Drakatos et al. (2002)

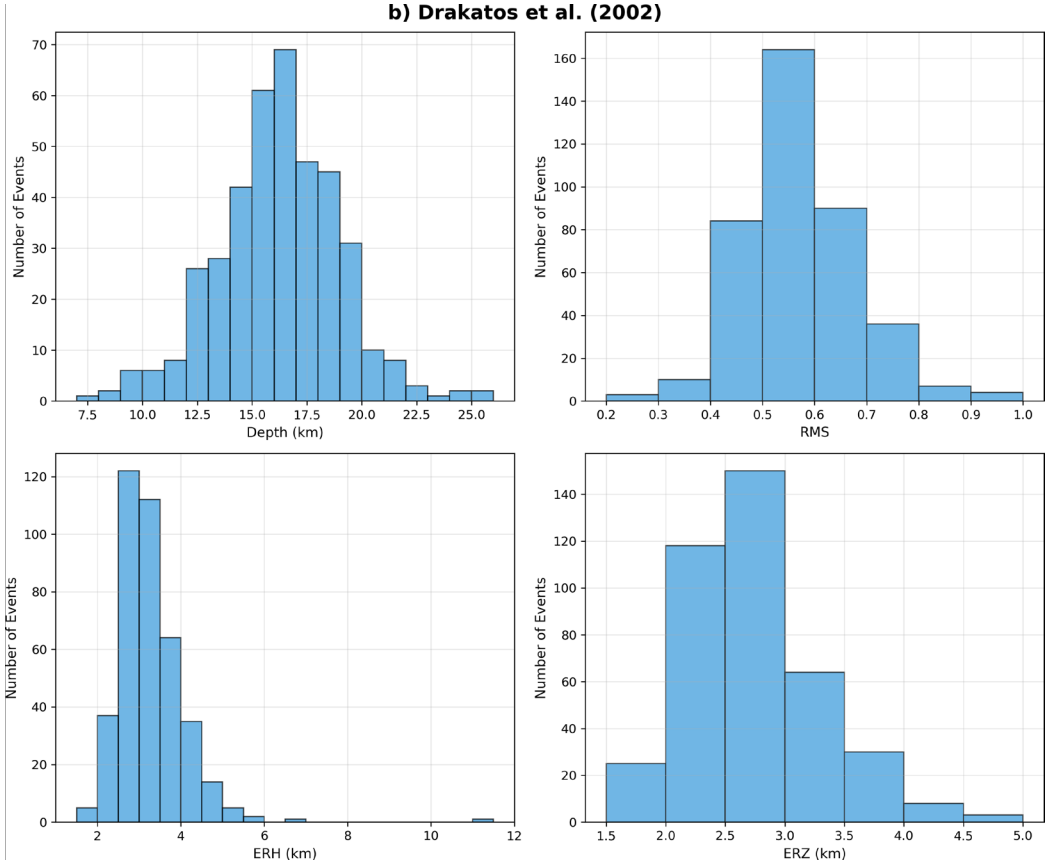

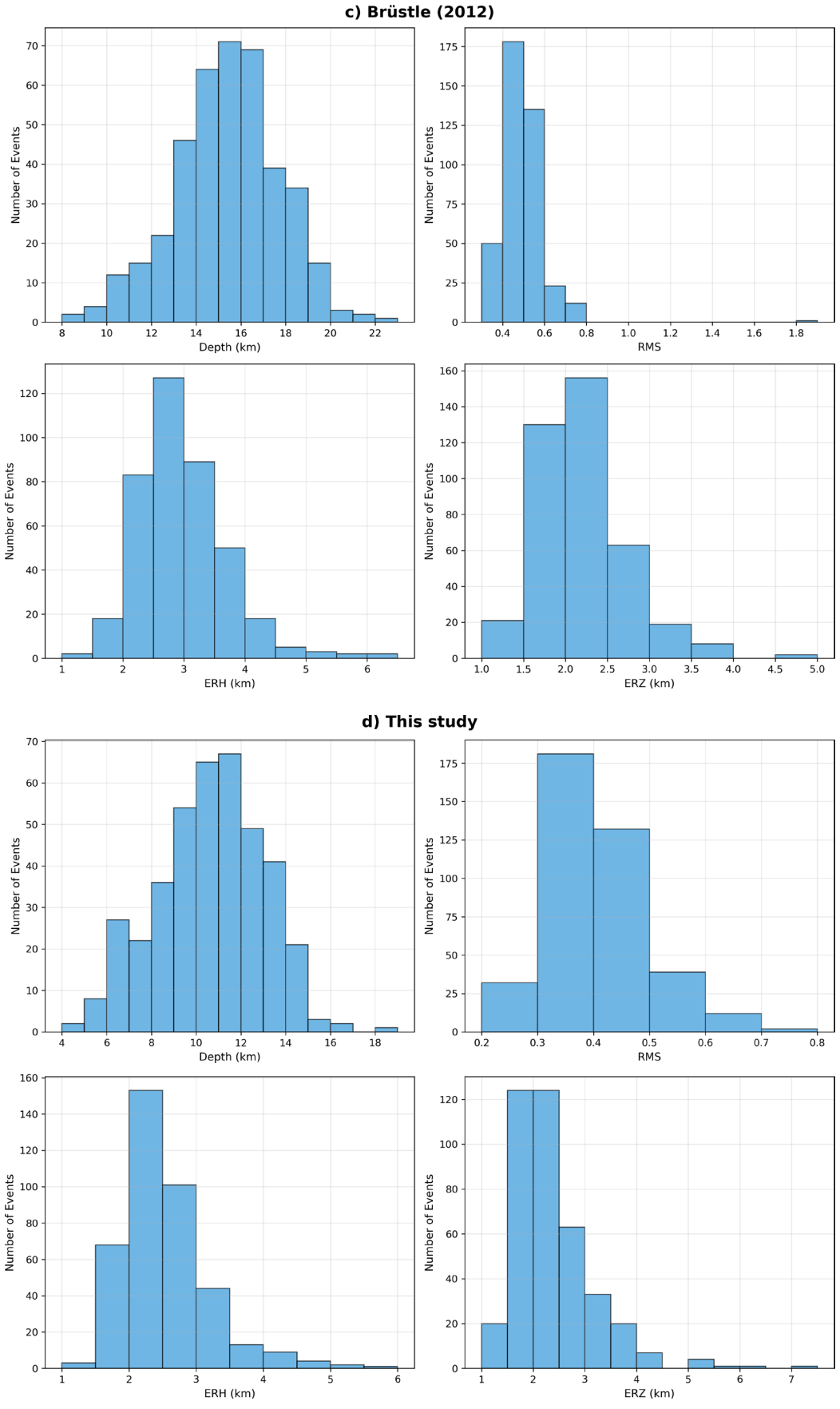

Figure 9. Comparison of the results obtained using different velocity models: (a) Novotny et al. (2001), (b) Drakatos et al. (2002), (c) Brüstle (2012), and (d) the velocity model developed in this study. Each panel presents the Depth, RMS, ERH, and ERZ parameters corresponding to the respective velocity model.

remain comparable, centered near 2-3 km, though with a few larger outliers. The Brüstle (2012) model also favors deeper hypocenters (14-16 km) similar to Drakatos, but provides lower RMS values (0.3-0.5 s) and slightly improved ERH/ERZ distributions, indicating a more stable fit and improved consistency of event locations.

In this study, the newly derived local 1D velocity model yields focal depths mostly between 8-13 km, representing an intermediate range between the shallow Novotny and deeper Drakatos-Brüstle models. The RMS residuals (0.3-0.4 s) are the lowest among all models, demonstrating a better fit between observed and calculated travel times. Similarly, both ERH and ERZ distributions show reduced horizontal and vertical uncertainties, peaking around 2 km, implying improved precision in earthquake locations. Overall, the results indicate that the local velocity model developed in this study enhances location accuracy and provides more realistic depth estimates consistent with the regional crustal structure.

4.1 Focal Mechanism Solution with the Computed Velocity Model

It is well known that employing an accurate velocity model in computation of the Green's function plays a crucial role in the inversion process. The impact of the velocity model and the corresponding variations on the resultant focal mechanism solutions are analyzed in several studies (Fojtikova et al., 2014; Dias et al., 2016; Turhan et al., 2018; Carvalho et al., 2018). Focal mechanism solution of one of the biggest earthquake in Aegean Sea seismic activity is calculated by the widely used ISOLA software package (Sokos and Zahradnik, 2006, 2008, 2013). This technique utilizes an iterative deconvolution inversion approach (Kikuchi and Kanamori, 1992) to solve for the best single- or multiple-point source representation for each earthquake. Hence, moment tensors are estimated by minimizing the least-squares misfit between observed and synthetic waveforms; sub-event positions and relative times are calculated through a grid search. In order to model a full wavefield at regional and local distances, Green's functions are calculated using the discrete wavenumber method.

The moment tensor solution for the 04 February 2025 (M5.0) earthquake is investigated to see the performance of the 1D velocity model calculated in this study. Figure 10 shows the moment tensor solution of this earthquake computed by using the velocity model previously documented (https://github.com/nikosT/Gisola/blob/d12156ff4cc6cc59594e6db2f22d6fde78c2fe03/src/crustals/karagianniS.vz#L4) in Gisola (Triantafyllis et al., 2021). Figure 11 shows the results of the same earthquake calculated with the velocity model computed in this study.

Focal mechanism solution of the biggest earthquake in Aegean Sea earthquake activity is calculated by widely used ISOLA software package (Sokos and Zahradnik, 2006, 2008, 2013). This technique utilizes an iterative deconvolution inversion (Kikuchi and Kanamori, 1992) to solve for the best single- or multiple-point source representation of each earthquake and hence moment tensors are estimated by a least-squares minimization of

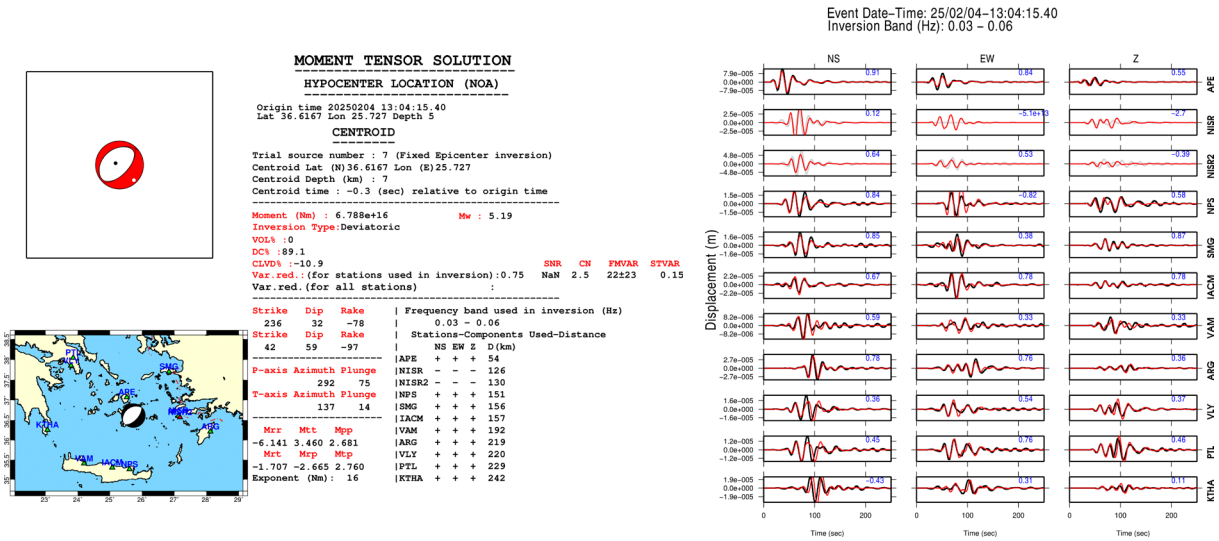

Figure 10. Results of the moment tensor solution parameters of the 04 February 2025 (M4.9) earthquake with the Green's functions computed by the test model defined in Gisola.

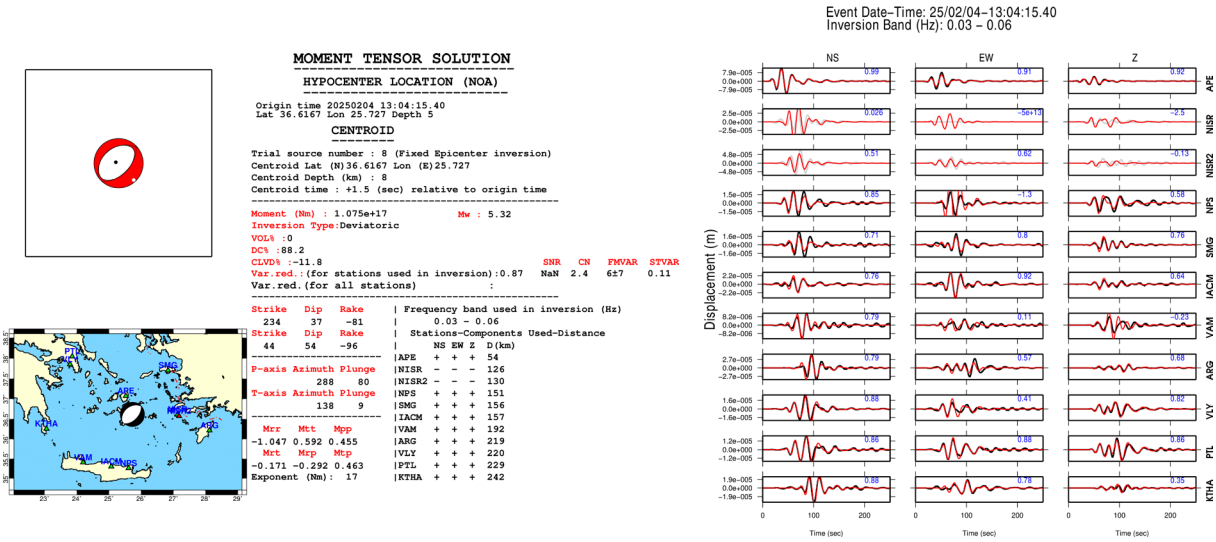

Figure 11. Results of the moment tensor solution parameters of the 04 February 2025 (M4.9) earthquake with the Green's functions computed by the velocity model estimated in this study (Table 2) and the observed versus synthetic waveform fits.

misfits between observed and synthetic waveforms; sub-event positions and relative times are calculated through grid search. In order to represent a full wavefield at regional and local distances, Green's functions are calculated using the discrete wavenumber method. The result to f the moment tensor solution for this event is also presented at the Moment Tensor Solutions' segment of the NOA web page (https://bbnet.gein.noa.gr/HL/seismicity/mts).

The results of the moment tensor solution in Fig. 10 and Fig. 11 indicate similar output parameters such as centroid depth (from 7 km to 8 km), CLVD component (−10.9, 11.8), CN (2.5, 2.4), STVAR (0.15, 0.11) mainly with slight improvements with the velocity model computed in this study (Fig. 11, Table 3). The most significant improvement in the outputs of the Fig. 11 were achieved in the variance reduction (VR = 0.87) and focal mechanism variability index (FMVAR (6 ± 7), when compared with the one solved in Fig. 10 (VR = 0.75, FMVAR = 22 ± 23).

5. Results and Conclusions

Determining accurate earthquake locations in regions with complex geological structures is often challenging due to uncertainties in seismic wave propagation and path effects. Nevertheless, precise event locations remain fundamental for routine seismic monitoring, source parameter estimation, and as an initial step toward three-dimensional tomographic studies.

This study utilized the seismic activity recorded in the Cyclades Archipelago during the 2025 earthquake sequence to develop a minimum 1D crustal velocity model. The objective was to assess the influence of this model on earthquake location parameters and moment tensor solutions. For the inversion, a dataset of 409 well-recorded earthquakes was selected, yielding a well-constrained minimum 1D velocity model. Considering the previously discussed differences in crustal structure and velocities between western and eastern Anatolia, the obtained velocity model exhibits higher velocities compared to the model derived for eastern Anatolia by Acarel et al. (2019), which was developed using the same methodology and data selection criteria. Both of these methods are in line with the reference earth models computed for eastern and western Anatolia (Cambaz, 2010).

In conclusion, the comparison of the velocity models indicates clear improvements achieved by the local 1D model developed in this study. While Novotny et al. (2001) produced shallower depths and Drakatos et al. (2002) and Brüstle (2012) yielded deeper hypocenters, the present model provides intermediate focal depths (8-13 km) that better reflect the expected seismogenic zone of the region. The RMS residuals (0.3-0.4 s) are the lowest among all models, and both horizontal and vertical errors are significantly reduced, enhancing the reliability of earthquake locations. These results demonstrate that the new velocity model offers a more accurate representation of the regional crustal structure and improves the overall quality and consistency of seismic event relocations.Relocation of these

earthquakes using the computed model resulted in improved event locations, with hypocentral depths generally becoming shallower. The average depth distribution peaks between 8 and 13 km, which corresponds to the estimated thickness of the brittle crust in the region. The distribution of relocated depths is in coincidence with the focal depths obtained in Fountoulakis and Evangelidis (2025) and Isken et al. (2025). The station delays obtained with the new model are consistent with the known crustal structure, confirming its reliability. The relocation results obtained using the optimal 1D velocity model and corresponding station corrections demonstrate a consistent adjustment for local geological effects. Negative corrections indicate higher seismic velocities, whereas positive ones reflect slower structures relative to the reference station. The distribution of station corrections, with lower values in the south and higher values in the north of the reference station (Anydros), suggests a lateral variation in crustal properties, highlighting the model's ability to capture regional velocity heterogeneity accurately.

Overall, the newly derived 1D velocity model provides a more realistic representation of the Cyclades crustal structure. By better capturing local geological and structural heterogeneities, it significantly enhances the precision of earthquake locations and moment tensor determinations. This model can therefore serve as a valuable reference for future seismological, source-mechanism, and crustal studies in the Aegean region.

While the current 1D velocity model marks a substantial improvement, it can be further refined with data from an expanded seismic network or enhanced earthquake catalogs. Moreover, incorporating additional datasets – such as ambient seismic noise measurements – or applying advanced techniques, including machine learning-based inversions, could yield more detailed and robust velocity models. Improved depth determinations, in turn, would provide better constraints for ground-motion modeling, fault kinematics, and the seismotectonic characterization of the study area.

Data availability statement. Data can be downloaded from the web page of National Observatory of Athens, Institute of Geodynamics: https://bbnet.gein.noa.gr/HL/databases/database (HL – National Observatory of Athens, Institute of Geodynamics, Athens (1975). National Observatory of Athens Seismic Network [Data set], FDSN, https://doi.org/10.7914/SN/HL.).

Acknowledgements. Earthquake and waveform catalogue data used in this study was obtained from the web page of National Observatory of Athens (NOA; https://bbnet.gein.noa.gr/HL/databases/database). Authors especially thanks to duty officers and the earthquake analysis team of NOA for providing data for this and other innumerable research papers. Some of the figures were made by using the Generic Mapping Tools (GMT) software (Wessel et al., 2013) and Obspy (Beyreuther et al., 2010). Data used in this study can be obtained from the web pages of NOA (https://bbnet.gein.noa.gr/HL/) and also from the web page of EIDA NOA Services (https://eida.gein.noa.gr/) (HL – National Observatory of Athens, Institute of Geodynamics, Athens (1975). National Observatory of Athens Seismic Network [Data set], FDSN, https://doi.org/10.7914/SN/HL). Finally, the authors sincerely thank to the Sector Editor Irene Molinari, an anonymous reviewer and the reviewer Irene Menichelli for their valuable and constructive feedback which significantly improved the submitted manuscript.

Reference

Acarel, D., M. D. Cambaz, F. Turhan, A. K. Mutlu and R. Polat (2019). Seismotectonics of Malatya Fault, Eastern Turkey, Open Geosci., 11, 1098-1111, doi:10.1515/geo-2019-0085.

Ambraseys, N. N. and J. A. Jackson (1990). Seismicity and associated strain of central Greece between 1890 and 1988, Geophys. J. Int., 101, 3, 663-708.

Acarel, D., M. D. Cambaz, F. Turhan, A. K. Mutlu et al. (2019). Seismotectonics of Malatya Fault, Eastern Turkey, Open Geosci., 11, 1098-1111, doi:10.1515/geo-2019-0085.

Antunes, V., T. Planes, J. Zahradník, A. Obermann et al. (2020). Seismotectonics and 1D velocity model of the Greater Geneva Basin, France-Switzerland, Geophys. J. Int. 221, 3, 2026-2047, doi:10.1093/gji/ggaa129.

Beyreuther, M., R. Barsch, L. Krischer, T. Megies et al. (2010). ObsPy: A Python toolbox for seismology, Seismol. Res. Lett. 81, 3, 530-533, doi:10.1785/gssrl.81.3.530.

Brüstle, A. (2012). Seismicity of the eastern Hellenic Subduction Zone. Ph.D. thesis, Ruhr University, Bochum, https://hss-opus.ub.ruhr-uni-bochum.de/opus4/frontdoor/deliver/index/docId/1127/file/diss.pdf.

Bohnhoff, M., J. Markis, D. Papanikolaou and G. Stavrakakis (2001). Crustal investigations of the Hellenic subduction zone using wide aperture seismic data, Tectonophysics, 343, 239-262.

Bohnhoff, M., M. Rische, T. Meier, D. Becker et al. (2006). Microseismic activity in the Hellenic Volcanic Arc, Greece, with emphasis on the seismotectonic setting of the Santorini-Amorgos zone, Tectonophysics, 423, 17-33.

Cambaz, M. D. (2010). Surface Wave Tomography of Turkey and Surroundings, PhD Thesis. p146, Bogazici University, Istanbul, Türkiye.

Cambaz, M. D. and H. Karabulut (2010). Love-wave group velocity maps of Turkey and surrounding regions, Geophys. J. Int. 181, 502-520.

Cambaz, M. D. and A. K. Mutlu (2016). Regional moment tensor inversion for Earthquakes in Turkey and its surroundings: 2008-2015, Seismol. Res. Lett., 87,5.

Cambaz, M. D., F. Turhan, M. Yılmazer, K. Kekovalı et al. (2019). An Investigation on the Evaluation of Seismic Network and Catalogue of Regional Earthquake-Tsunami Monitoring Center (RETMC-KOERI), Yerbilimleri, 40, 110-135.

Carvalho, J., L. V. Barros and J. Zahradnik (2018). Inversion for focal mechanisms using waveform envelopes and inaccurate velocity models: Examples from Brazil, Bull. Seism. Soc. Am., 2018, 109, 1, 138-151.

Delph, J. R., C. B. Biryol, S. L. Beck, G. Zandt and K. M. Ward. (2015). Shear wave velocity structure of the Anatolian Plate: Anomalously slow crust in southwestern Türkiye, Geophys. J. Int., 202, 1, 261-276, doi:10.1093/gji/ggv141.

Dewey, J. F., M. R. Hempton, W. S. F. Kidd, F. Şaroğlu et al. (1986). Shortening of continental lithosphere: the neotectonics of Eastern Anatolia – a young collision zone. In "Collision Tectonics", eds. M. P. Coward and A. C. Ries. Geol. Soc. Spec. Publ., 19, London. 3-36.

Dias, F., J. Zahradník and M. Assumpcao (2016). Path-specific, dispersion based velocity models and moment tensors of moderate events recorded at few distant stations: Examples from Brazil and Greece, J. South Am. Earth Sci., 71, 344-358.

Drakatos, G., G. Karantonis and G. Stavrakakis (1997). P-wave crustal tomography of Greece with use of an accurate two-point ray tracer, Annali di Geofisica, XL, 1, 25-36.

Drakatos, G., N. Melis, D. Papanastassiou, V. Karastathis et al. (2002). 3-D crustal velocity structure from inversion of local earthquake data in Attiki (central Greece) region, Natural Hazards, 27, 1-14.

Emre, Ö., T. Y. Duman, S. Özalp, H. Elmacı et al. (2013). Active Fault Map of Turkey, General Directorate of Mineral Research and Exploration, Ankara, Türkiye.

Emre, Ö., T. Y. Duman, S. Özalp and F. Şaroğlu (2018). Active fault Database of Turkey. B Earthq Eng, 16, 8, 3229-3275.

Evangelidis, C. P., N. Triantafyllis, M. Samios, K. Boukouras et al. (2021). Seismic Waveform Data from Greece and Cyprus: Integration, Archival, and Open Access, Seismol. Res. Lett. XX, 1-13, doi:10.1785/0220200408.

Fojtikova, L. and J. Zahradnik (2014). A new strategy for weak events in sparse networks: the first-motion polarity solutions constrained by single-station waveform inversion, Seism. Res. Lett., 85, 1265-1274.

Fountoulakis, I. and C. P. Evangelidis (2025). The 2024-2025 seismic sequence in the Santorini-Amorgos region: Insights into volcano-tectonic activity through high-resolution seismic monitoring. Seismica, 4, 1, doi:10.26443/seismica.v4i1.1663.

Ganas, A., I. A. Oikonomou and C. Tsimi (2013). NOAfaults: a digital database for active faults in Greece. Bulletin of the Geological Society of Greece, 47, 2, 518-530, Δελτίο Ε.Γ.Ε., τόμος XLVII – 13ο Διεθνές Συνέδριο της Ελληνικής Γεωλογικής Εταιρίας, Χανιά, 5-8 Σεπτεμβρίου, 518-530, doi:10.12681/bgsg.11079.

Ganas, A., V. Tsironi, E. Kollia, M. Delagas et al. (2018). Recent upgrades of the NOA database of active faults in Greece (NOAFAULTs). 19th General Assembly of WEGENER, September 2018, Grenoble, https://wegener2018.sciencesconf.org/.

Ganas, A., V. Tsironi, E. Efstathiou, E. Konstantakopoulou et al. (2023). The National Observatory of Athens active faults of Greece database (NOAFAULTs) version 2023. In: Book of Abstracts of the 8th International Colloquium on Historical Earthquakes, Palaeo-Macroseismology and Seismotectonics, Bull. Geol. Soc. Special Pub., 11, 36-38, ISBN: 978-618-86841-1-9.

Gomberg, J. S., M. Kaye, S. Shedlock and W. Roecker (1990). The effect of S-wave arrival times on the accuracy of hypocenter estimation, Bull. Seismol. Soc. Am., 80, 6A, 1605-1628, doi:10.1785/BSSA08006A1605.

Havskov, J. and L. Ottemöller (1999). SeisAn Earthquake analysis software, Seis. Res. Lett., 70, 5, 532-534.

Hetényi, G., I. Molinari, J. Clinton et al. (2018). The AlpArray Seismic Network: A Large-Scale European Experiment to Image the Alpine Orogen, Surv. Geophys., 39, 1009-1033, doi:10.1007/s10712-018-9472-4.

Howell, A., J. Jackson, A. Copley, D. McKenzie and E. Nissen (2017). Subduction and vertical coastal motions in the eastern Mediterranean, Geophys. J. Int., 211, 1, 593-620, doi:10.1093/gji/ggx307.

Husen, S., E. Kissling and J. F. Clinton (2011). Local and regional minimum 1D models for earthquake location and data quality assessment in complex tectonic regions: application to Switzerland, Swiss J. Geosci., 104, 3, 455-469.

HL – National Observatory of Athens, Institute of Geodynamics, Athens (1975). National Observatory of Athens Seismic Network [Data set], FDSN, doi:10.7914/SN/HL.

Isken, M. P., J. Karstens, P. Nomikou et al. (2025). Volcanic crisis reveals coupled magma system at Santorini and Kolumbo, Nature 645, 939-945, doi:10.1038/s41586-025-09525-7.

Jackson, J. and D. McKenzie (1988). The relationship between plate motions and seismic moment tensors, and the rates of active deformation in the Mediterranean and Middle East, Geophysical Journal International, Volume 93, Issue 1, April, Pages 45-73, doi:10.1111/j.1365-246X.1988.tb01387.x.

James, D. E., I. S. Sacks, L. E. Lazo and G. P. Aparicio (1969). On locating local earthquakes using small networks, Bull. Seismol. Soc. Am., 59, 3, 1201-1212, doi:10.1785/BSSA0590031201.

Karagianni, E., D. Panagiotopoulos, G. Panza, P. Suhadolc et al. (2002). Rayleigh wave group velocity tomography in the Aegean area, Tectonophysics, 358,187-209.

Karagianni, E., C. Papazachos, D. Panagiotopoulos, P. Suhadolc et al. (2005). Shear velocity structure in the Aegean area obtained by inversion of Rayleigh waves, Geophys. J. Int., 160, 127-143.

Karagianni, E. and C. Papazachos (2007). Shear velocity structure in the Aegean region obtained by joint inversion of Rayleigh and Love waves, in T. Taymaz, Y. Yilmaz and Y. Dilek (eds). The Geodynamics of the Aegean and Anatolia, Geological Society, London, Special Publications, 291, 159-181.

Kianimehr, H., E. Kissling, F. Yaminifard et al. (2018). Regional minimum 1-D P-wave velocity model for a new seismicity catalogue with precise and consistent earthquake locations in southern Iran, J. Seismol., 22, 1529-1547. doi:10.1007/s10950-018-9783-4.

Kikuchi, M. and H. Kanamori (1992). Inversion of complex body waves-III, Bull. Seismol. Soc. Am., 81, 2335-2350.

Kissling, E. (1988). Geotomography with local earthquake data, Rev. Geophys., 26, 659-698.

Kissling, E., W. L. Ellsworth, D. Eberhart-Philips and U. Kradolfer (1994). Initial reference models in seismic tomography, J. Geophys. Res., 99, 19635-19646.

Kissling, E., U. Kradolfer and H. Maurer (1995). VELEST User's Guide, https://seg.ethz.ch/software/velest.html.

Kolínský, P., T. Meier, M. R. Agius, A. Bijedić, G. Bokelmann, F. Borleanu et al. (2025). AdriaArray – a Passive Seismic Experiment to Study Structure, Geodynamics and Geohazards of the Adriatic Plate, Ann. Geophys, 68, this issue, doi:10.4401/ag-9284.

Konstantinou, K. I. (2018). Estimation of optimum velocity model and precise earthquake locations in NE Aegean: Implications for seismotectonics and seismic hazard, J. Geodyn.,121, 143-154, doi:10.1016/j.jog.2018.07.005.

Le Pichon, X. and J. Angelier (1979). The Hellenic arc and trench system: A key to the neotectonic evolution of the eastern Mediterranean area, Tectonophysics, 60, 1-2, 1-42, doi:10.1016/0040-1951(79)90131-8.

Lienert, B. R., E. Berg and L. Neil Frazer. (1986). HYPOCENTER: An earthquake location method using centered, scaled, and adaptively damped least squares, Bull. Seismol. Soc. Am.; 76, 3, 771-783. doi:10.1785/BSSA0760030771.

Lienert, B. R. and J. Havskov (1995). A computer program for locating earthquakes both locally and globally, Seismol. Res. Lett., 66, 26-36.

Makris, J. (1978). The crust and upper mantle of the Aegean region from deep seismic soundings, Tectonophysics, 46, 269-284.

McKenzie, D. (1972). Active tectonics of the Mediterranean region, Geophys. J. R. Astr. Soc., 30, 109-185.

McKenzie, D. P. (1978). Active tectonics of the Alpine-Himalayan belt: the Aegean Sea and surrounding regions, Geophys. J. R. Astr. Soc., 55, 217-354.

Okal, E., C. Synolakis, B. Uslu, N. Kalligeris and E. Voukouvalas (2009). The 1956 earthquake and tsunami in Amorgos, Greece, Geophys. J. Int., 178, 1533-1554.

Okay, A. I. and O. Tuysuz (1999). Tethyan sutures of northern Turkey, in "The Mediterranean Basins: Tertiary Extension within the Alpine orogen", 475-515, eds B. Durand, L. Jolivet, F. Horv´ath and M. S´eranne, Geological Society, Special Publication 156 London.

Ottemöller, V. and J. Havskov (2013). SEISAN Earthquake Analysis Software for Windows, Solaris, Linux and Macosx.

Papadopoulos, G. A. and S. B. Pavlides (1992). The 1956 large shock in the South Aegean: Macroseismic field, faulting and neotectonics of the Amorgos Island, Earth Planet. Sci. Lett., 113, 383-396.

Papazachos, B. and G. Nolet (1997). P and S deep velocity structure of the Hellenic area obtained by robust nonlinear inversion of travel times, J. Geophys. Res., 102, B4, 8349-8367.

Pavlides, S., G. Drakatos and N. Zouros (2024). Active Tectonics and Seismicity in Greece. In: R. Darques, G. Sidiropoulos and K. Kalabokidis (eds) The Geography of Greece. World Regional Geography Book Series. Springer, Cham. doi:10.1007/978-3-031-29819-6_25.

Piromallo, C. and A. Morelli (2003). P wave tomography of the mantle under the Alpine-Mediterranean area, J. Geophys. Res., 108, B2, 2065, doi:10.1029/2002JB001757.

Reilinger, R. et al. (2006). GPS constraints on continental deformation in the Africa-Arabia-Eurasia continental collision zone and implications for the dynamics of plate interactions, J. Geophys. Res., 111, B05411, doi:10.1029/2005JB004051.

Saunders, P., K. Priestley and T. Taymaz. (1998). Variations in the crustal structure beneath western Türkiye, Geophys. J. Int., 134, 2, 373-389, doi:10.1046/j.1365-246x.1998.00571.x.

Sodoudi, F. et al. (2006). Lithospheric structure of the Aegean obtained from P and S receiver functions, J. Geophys. Res., 111, B12307, doi:10.1029/2005JB003932.

Stampfli, G. M. (2000). Tethyan Oceans, in Tectonic and Magmatism in Turkey and the Surrounding Area, Vol. 173, eds Bozkurt, E., J. A. Winchester and J. D. A. Piper, pp. 1-23, Geological Society, Special Publications, London.

Salaün, G., H. A. Pedersen, A. Paul, the SIMBAAD Team et al. (2012). High-resolution surface wave tomography beneath the Aegean-Anatolia region: constraints on upper-mantle structure, Geophys J. Int., 190, 406-420, doi:10.1111/j.1365-246X.2012.05483.x.

Sokos, E. and J. Zahradnik (2006). A MATLAB GUI for Use with ISOLA Fortran Codes User's Guide, http://seismo.geology.upatras.gr/isola/.

Sokos, E. and J. Zahradník (2008). ISOLA a Fortran code and a Matlab GUI to perform multiple-point source inversion of seismic data, Comput. Geosci., 34, 967-977, doi:10.1016/j.cageo.2007.07.005.

Sokos, E. and J. Zahradník (2013). Evaluating centroid-moment tensor uncertainty in the new version of ISOLA software, Seismol. Res. Lett., 2013, 84, 656-665, doi:10.1785/0220130002.

Sokos, E., C. Evangelidis, G. Kaviris and C. Papazachos (2023). AdriaArray station installations in Greece. ion AdriaArray International Workshop 2023, 3-5 April 2023 Dubrovnik Croatia.

Tatar, O., J. D. Piper and H. Gursoy (2000). Paleomagnetic study of the Erciyes sector of the Ecemis¸ Fault Zone: neotectonic deformation in the southeastern part of the anatolian Block; in Tectonics and Magmatism in Turkey and the Surrounding Area,173, 423-440, eds E. Bozkurt, J. A. Winchester and J. D. A., Piper, Geological Society, Special Publications, London.

Taymaz, T., J. A. Jackson and R. Westaway (1990). Earthquake mechanisms in the Hellenic trench near Crete, Geophys. J. Int., 102, 695-731.

Taymaz, T., J. A. Jackson and D. McKenzie (1991). Active tectonics of the north and central Aegean Sea, Geophys. J. Int., 106, 2, 433-490.

Thurber, C. H. (1992). Hypocenter-velocity structure coupling in local earthquake tomography, Phys. Earth and Planet. Inter., 75, 1-3, 55-62, doi:10.1016/0031-9201(92)90117-E.

Tirel, C., F. Gueydan, C. Tiberi and J.-P. Brun (2004). Aegean crustal thickness inferred from gravity inversion. Geodynamical implications, Earth Planet. Sci. Lett., 228, 267-280.

Triantafyllis, N., E. I. Venetis, I. Fountoulakis, E-V. Pikoulis et al. (2021). Gisola: A High-Performance Computing Application for Real-Time Moment Tensor Inversion, Seismol. Res. Lett., 93, 2A, 957-966. doi:10.1785/0220210153.

Triantafyllou, I. and G. Papadopoulos (2025). A unique seismic cluster near Santorini, Greece, foreshadows a strong earthquake? https://static1.emsc.eu/Doc/Additional_Earthquake_Report/1762480/Santorini%20report.pdf.

Turhan, F., M. D. Cambaz and J. Zahradník. (2018). The significance of the crustal velocity model in moment tensor solutions: A case study of Yedisu earthquakes. In: "Moment Tensor Solutions – A Useful Tool for Seismotectonics" (S. D'Amico, Ed.), Springer.

Wessel, P., W. H. F. Smith, R. Scharroo, J. Luis et al. (2013). Generic mapping tools improved version released. EOS Trans. Am, Geophys. Union, 94, 409-410, doi:10.1002/2013EO450001.

***CORRESPONDING AUTHOR: Musavver DIDEM CAMBAZ**,
Boğaziçi University, Kandilli Observatory and Earthquake Research Institute, 34684, Çengelköy, Üsküdar, İstanbul, Türkiye
e-mail: didem.samut@bogazici.edu.tr